Kinetics of yttrium oxide carbochlorination

J.P. Gaviría [a,b,*], G.G. Fouga [a,b], A.E. Bohé [a,b,c]

[a] División Cinética Química - Complejo Tecnológico Pilcaniyeu - Centro Atómico Bariloche - Comisión Nacional de Energía Atómica, Av. Bustillo km 9500 (8400), S.C. de Bariloche, Río Negro, Argentina
[b] Consejo Nacional de Investigaciones Científicas y Técnicas, Argentina
[c] Centro Regional Universitario Bariloche - Universidad Nacional del Comahue, Argentina

ABSTRACT

The chlorination kinetics of the Y_2O_3–sucrose carbon system was studied by thermogravimetry. This work is a continuation of a previous one in which the reaction stages and the stoichiometry of each reaction have been determined. The influence of carbon content, total flow rate, sample initial mass and chlorine partial pressure was evaluated. The effect of carbon content on the reactive mixture was studied between 6.7 and 70% (carbon mass/total mass). The results showed that the reaction rate of each stage is strongly increased as the carbon content increases and the range of occurrence of the stages depends on the amount of carbon in the solid reactive mixture. The formation reaction of YOCl (*STAGE I*) is chemically controlled for temperatures lower than 700 °C with average effective activation energies of 165 ± 6 and 152 ± 7 kJ/mol for 8.7 and 16.7%C, respectively. The formation of the YOCl follows a nucleation and growth mechanism, with a combination of continuous nucleation and site saturation, and anisotropic growth controlled by diffusion. The kinetics of *STAGE I* can be expressed by the following global rate equation that includes the variables analyzed:

$$\frac{d\alpha}{dt} = k_0 B \exp\left(-\frac{Ea}{R_g T}\right) pCl_2 \{n(1-\alpha)[-\ln(1-\alpha)]\}^{(n-1)/n}$$

where $k_0 B = 1.9 \times 10^4$, $n = 1.20$ for 8.7%C, and $k_0 B = 8.4 \times 10^3$, $n = 1.14$ for 16.7%C.

STAGES II and *III* correspond to the YOCl carbochlorination to form YCl_3, being these stages kinetically different. It was not possible to obtain kinetic parameters for these stages. The reaction rate of *STAGE II* is affected by diffusion of Cl_2 through the gas film surrounding the sample and mass changes in *STAGE III* have two opposite components: formation and evaporation of liquid YCl_3.
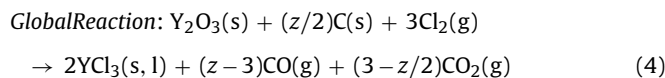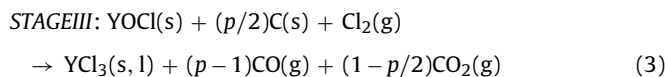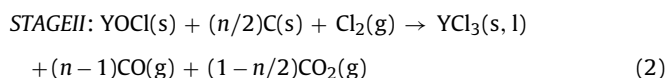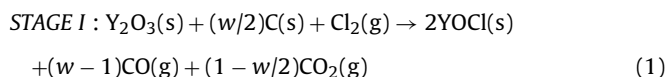
© 2011 Elsevier B.V. All rights reserved.

1. Introduction

In a work recently published [1] we have studied the chlorination reaction of a mixture composed by Y_2O_3 and sucrose carbon (C). It was concluded that the reaction progresses through three successive stages until the complete formation of YCl_3. The occurrences of these stages depend on the temperature and carbon content. Fig. 1 shows a thermogravimetric curve obtained in the Y_2O_3–C (30%) chlorination at 750 °C. *STAGE I* consists of the Y_2O_3 carbochlorination to produce YOCl, and *STAGES II* and *III* correspond to the YOCl carbochlorination to form YCl_3 (which is liquid at 750 °C, $Tf_{YCl_3} = 685$ °C [1]). The difference between these last stages is the kinetic nature, being called fast and slow, respectively.

The reactions in each stage are the followings:

STAGE I : $Y_2O_3(s) + (w/2)C(s) + Cl_2(g) \rightarrow 2YOCl(s)$
$$+ (w-1)CO(g) + (1-w/2)CO_2(g) \quad (1)$$

STAGE II: $YOCl(s) + (n/2)C(s) + Cl_2(g) \rightarrow YCl_3(s, l)$
$$+ (n-1)CO(g) + (1-n/2)CO_2(g) \quad (2)$$

STAGE III: $YOCl(s) + (p/2)C(s) + Cl_2(g)$
$$\rightarrow YCl_3(s, l) + (p-1)CO(g) + (1-p/2)CO_2(g) \quad (3)$$

Global Reaction: $Y_2O_3(s) + (z/2)C(s) + 3Cl_2(g)$
$$\rightarrow 2YCl_3(s, l) + (z-3)CO(g) + (3-z/2)CO_2(g) \quad (4)$$

where $1 \leq w, n, p \leq 2$ and $3 \leq z \leq 6$.

* Corresponding author at: División Cinética Química - Complejo Tecnológico Pilcaniyeu - Centro Atómico Bariloche - Comisión Nacional de Energía Atómica, Av. Bustillo km 9500 (8400), S.C. de Bariloche, Río Negro, Argentina.
Tel.: +54 02 94 444 5100; fax: +54 02 94 444 5293.
E-mail addresses: gaviriaj@cab.cnea.gov.ar, juanpablogaviria@yahoo.com.ar (J.P. Gaviría).
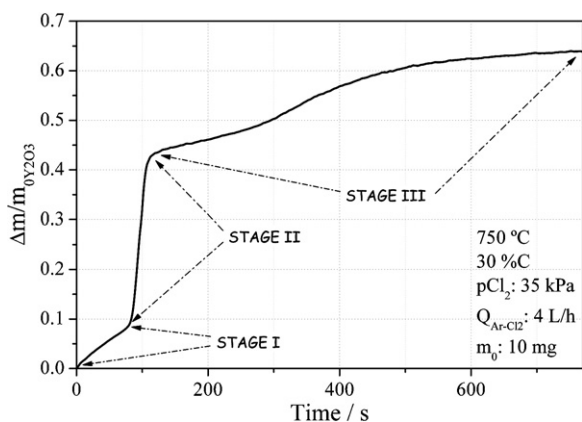
Fig. 1. Reaction stages in the chlorination of Y_2O_3–C.

Fig. 2. Effect of the carbon content in the chlorination of Y_2O_3–C. (a) 600 °C and (b) 750 °C.

The stoichiometries of the *STAGE I* and *Global Reaction* were calculated from mass balances obtaining $w = 1.16(600–650 °C)$ and $z = 4(725–775 °C)$ [1]. In order to perform these calculations the interaction between sucrose carbon and chlorine was analyzed by thermogravimetry and it was quantified the amount of chlorine which is adsorbed on the carbon surface. The aim of the present work is the kinetic study of the stages involved in the overall reaction.

2. Materials and methods

Solid reactants used were an yttrium oxide powder 99.99% (Aldrich Chemical Company, Inc., Milwaukee, MI) and sucrose carbon. The mean particle size of the oxide measured by laser diffraction was 10 μm and showed a size distribution highly homogeneous (Mastersizer, Malvern Instruments Limited, Worcestershire, UK) [2]. Carbon was obtained from the pyrolysis of sucrose (Fluka Chemie AG) in inert atmosphere at 980 °C during 48 h and sieved to a size of 400 mesh (ASTM, square aperture of 37 μm). Carbon characteristics are well described by González et al. [3]. Amorebieta and Colussi [4] and Pasquevich [5] utilized sucrose carbon and determined by mass spectroscopy that this type of carbon does not have volatile organic residues at the reaction conditions. The oxide and carbon powder have a BET surface area of 3.7 and 7.2 m²/g, respectively (Digisorb 2600 Micrometeritics Instrument, Norcross, GA). Respective amounts of the solid reactants were weighed and mixed mechanically to obtain Y_2O_3–C mixtures in the range of 6.7–70% (wt/wt, carbon mass/total mass). The kinetic analysis were performed with mixtures of 8.7%C (carbon is 20% in excess with respect to the stoichiometry of reaction (1) with only $CO_2(g)$ as gas product) and 16.7%C (carbon is 20% in excess with respect to the stoichiometry of reaction (1) with only $CO(g)$ as gas product).

Gases used were Cl_2 99.8% purity (Indupa, Bahía Blanca, Argentina) and Ar 99.99% purity (AGA, Buenos Aires, Argentina).

Solids were analyzed by X-ray diffraction (XRD) (Philips PW 1310-01) and scanning electron microscopy (SEM) (SEM 515, Philips Electronic Instruments).

The chlorinations reactions were performed using a thermogravimetric system, which has been described elsewhere [6]. It consists of an electrobalance (Cahn 2000, Cahn Instruments, Inc., Cerritos, CA) adapted to work with corrosive atmospheres, a vertical tube furnace, a gas line, and a data acquisition system. The sensitivity of the system is ±5 μg while operating at 1000 °C under a gas flow rate of 9 L/h, measured at normal temperature and pressure. Each sample was placed in a cylindrical quartz crucible (7.8-mm inner diameter and 3.3-mm deep), which hangs from one of the arms of the electrobalance through a quartz wire. A quartz
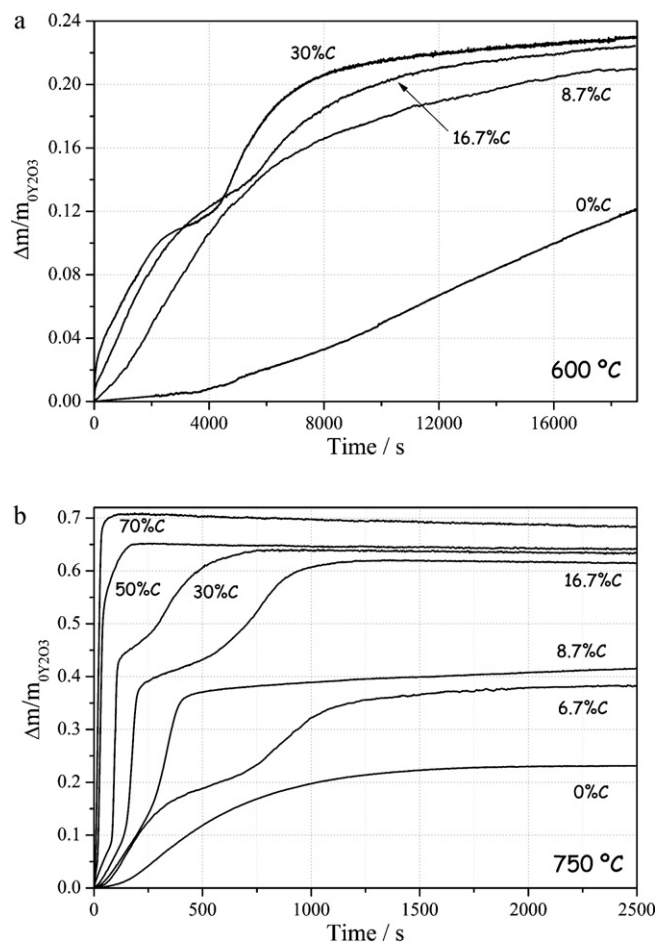
hangdown tube (4.6-cm diameter) carried the gases to the sample. The temperature of the sample was measured using a Pt–Pt (10% Rh) thermocouple encapsulated in quartz, which was placed 2 mm below the crucible. Flows of Ar and Cl_2 were controlled by means of flow meters and they were dried by passing through silica gel and $CaCl_2$, respectively. The Y_2O_3–C samples were heated in flowing Ar until the reaction temperature was reached. After temperature stabilization, chlorine was admitted into the hangdown tube while mass changes were continuously monitored (the mass changes were acquired every 2.5 s). The acquired data of mass and time were carefully analyzed to determine the reaction zero time.

3. Results and discussion

3.1. Influence of carbon content

Fig. 2 shows the thermogravimetries of chlorinations of Y_2O_3–C mixtures with carbon contents between 0 and 70% at 600 and 750 °C, keeping the other experimental conditions ($Q_{Ar–Cl_2}$: 4 L/h, m_0: 10 mg and pCl_2: 35 kPa). These curves indicate that the carbon content has a noticeable influence on kinetics and reaction phenomenology.

The XRD analysis of final products of the reactions at 600 °C gave YOCl as only phase present. The curves show that the rate was increased as the carbon content was increased, being more evident for %C lower than 16.7. The mixtures with %C lower than 8.7 proceed with mass gain until complete YOCl formation through *STAGE I*. The samples of 16.7 and 30%C react according to *STAGE I* until the shoulder placed at $\Delta m/m_{0Y_2O_3} \approx 0.11$ and 0.13, respectively. After
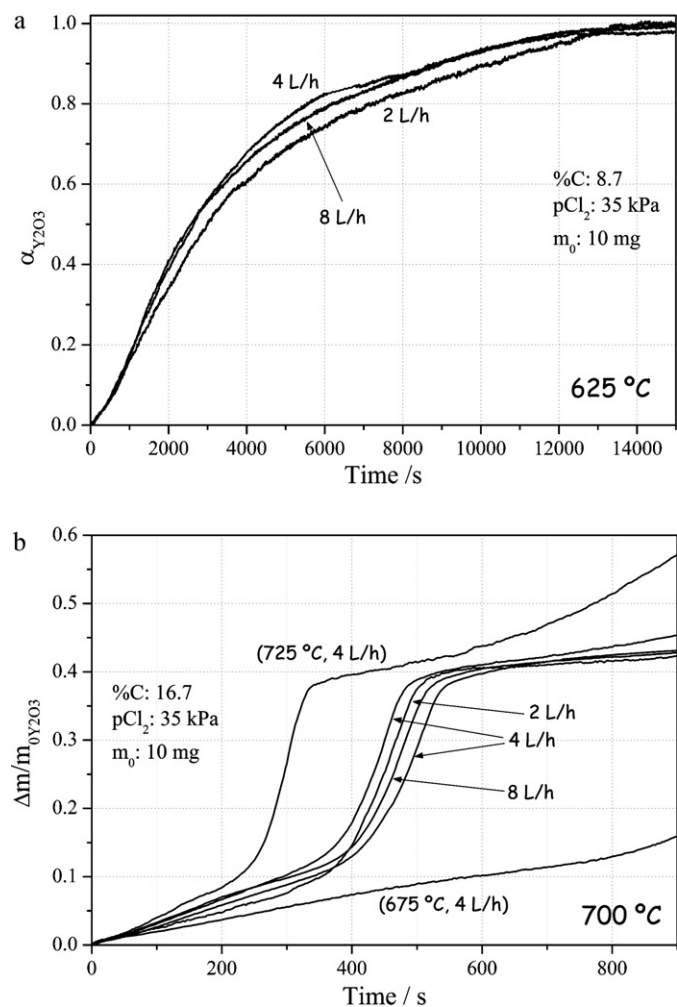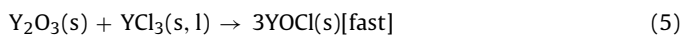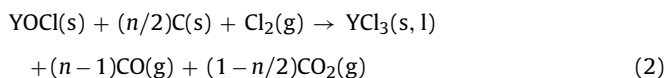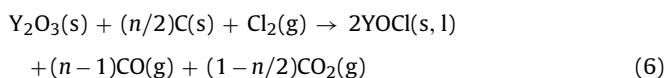
Fig. 3. Effect of flow rate of Ar–Cl$_2$ on the carbochlorination rate of Y$_2$O$_3$. (a) 625 °C and (b) 700 °C.

the shoulder, *STAGES I* and *II* occur simultaneously. The YOCl formed in the *STAGE I* is carbochlorinated producing solid YCl$_3$, which reacts quickly with non-reacted Y$_2$O$_3$ to form YOCl. The reactions involved are the followings:

$$YOCl(s) + (n/2)C(s) + Cl_2(g) \rightarrow YCl_3(s, l)$$
$$+ (n-1)CO(g) + (1-n/2)CO_2(g) \qquad (2)$$

$$Y_2O_3(s) + YCl_3(s, l) \rightarrow 3YOCl(s)[fast] \qquad (5)$$

Being the stoichiometry of the global reaction:

$$Y_2O_3(s) + (n/2)C(s) + Cl_2(g) \rightarrow 2YOCl(s, l)$$
$$+ (n-1)CO(g) + (1-n/2)CO_2(g) \qquad (6)$$

This reaction mechanism contributes to the formation of YOCl produced by the direct carbochlorination of Y$_2$O$_3$ (reaction (1)), causing an increase of the global mass gain rate.

The standard Gibbs free energy of reaction (5) has the following dependence on the temperature [7]:

$$\Delta G^0 = -85.15 + 0.0255 \times T(kJ/mol) \quad [500-700 °C] \qquad (I)$$

$$\Delta G^0 = -118.85 + 0.0588 \times T(kJ/mol) \quad [750-1000 °C] \qquad (II)$$

The ΔG^0 value is negative in all the temperature range used in this work, being −62.9 and −58.7 kJ/mol at 600 and 750 °C, respectively. The occurrence of reaction (5) was verified by heating in

Table 1
Values of relative mass gain of *STAGE II–III* transitions for the curves of Fig. 2 (750 °C).

| %C	STAGE II–III transition	
	$\Delta m/m_{0Y_2O_3}$ measured	$\Delta m/m_{0Y_2O_3}$ corrected by Cl$_2$–C interaction
6.7	0.353	0.350
8.7	0.373	0.369
16.7	0.384	0.376
30	0.434	0.416
50	0.545	0.503
70	Reaction proceeds through *STAGE II* until complete formation of YCl$_3$	

argon atmosphere mixtures of Y$_2$O$_3$–YCl$_3$ at 640 and 700 °C. The XRD analysis of the final products showed in both cases the formation of YOCl.

Fig. 2b shows the thermogravimetric curves of the reactive system Y$_2$O$_3$–C–Cl$_2$ at 750 °C. The sample without carbon experiences a mass gain until reach a final value of $\Delta m/m_{0Y_2O_3}$ corresponding to the total formation of YOCl. In the samples carbochlorinated the oxide is transformed into YOCl via *STAGE I* and later the oxychloride is carbochlorinated producing liquid YCl$_3$ via *STAGE II*. The beginning of the *STAGE II* depends on the carbon content, starting at lower relative mass change as the carbon content increase. *STAGE II* begins at $\Delta m/m_{0Y_2O_3} = 0.2, 0.15, 0.09, 0.08, 0.05$ and 0.02 for %C = 6.7, 8.7, 16.7, 30, 50 and 70, respectively. The curves do not take into account the chlorine adsorbed on the carbon surface [1], therefore the true values for $\Delta m/m_{0Y_2O_3}$ are smaller than those given above, and they are smaller as the %C is increased.

The start of the *STAGE III* is also affected by the carbon content, but unlike *STAGE I–II* transition, in this case the beginning of the next stage occurs at higher $\Delta m/m_{0Y_2O_3}$ values as the carbon content increases. Therefore, correction for chlorine adsorption by unreacted carbon has to be made in order to get a correct analysis of the carbon content influence. Table 1 shows the $\Delta m/m_{0Y_2O_3}$ values taken from the thermogravimetries in the *STAGE I–II* transition, and the values corrected by the Cl$_2$–C interaction. The calculations were performed according to the results obtained for the maximum relative mass gain experienced by the sucrose carbon in the interaction with chlorine [1] and were applied to the initial total carbon mass (in this way the results are conservatives).

The results show that even taking into account the Cl$_2$–C interaction, *STAGE II* is extended when the carbon content increases, and the mixture with 70%C progress through *STAGE II* until the complete formation of YCl$_3$.

The final samples (exposed to atmosphere) of reactions showed in Fig. 2b were analyzed by XRD, obtaining the following compounds: YOCl (0%C), YOCl + YCl$_3$·6H$_2$O (6.7%C), YCl$_3$·6H$_2$O (%C ≥ 8.7). Yttrium chloride was produced anhydrous inside the reactor, and it was hydrated when it was exposed to atmosphere [1]. The final product of the Y$_2$O$_3$ carbochlorination with 6.7%C was not completely YCl$_3$ due to the carbon content was in defect respect to the stoichiometry of the following reaction, which requires the minimum carbon content for producing YCl$_3$ by carbochlorination of Y$_2$O$_3$ [reaction (4) with z = 3]:

$$Y_2O_3(s) + 3/2C(s) + 3Cl_2(g) \rightarrow 2YCl_3(s, l) + 3/2CO_2(g) \qquad (7)$$
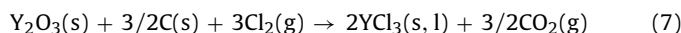
The behaviour observed for the carbon content influence can be explained by taking into account the thermodynamic and kinetic effects of the sucrose carbon. *STAGE II* progresses through the gaseous intermediate species produced in the Cl$_2$–C interaction. As higher carbon content in the reactive mixture, higher are the number of intermediate species and the extent of this stage. Once the intermediates are consumed the system behaves in a different way according to the temperature and carbon content. If the temperature is higher than the melting point of YCl$_3$ (685 °C) and
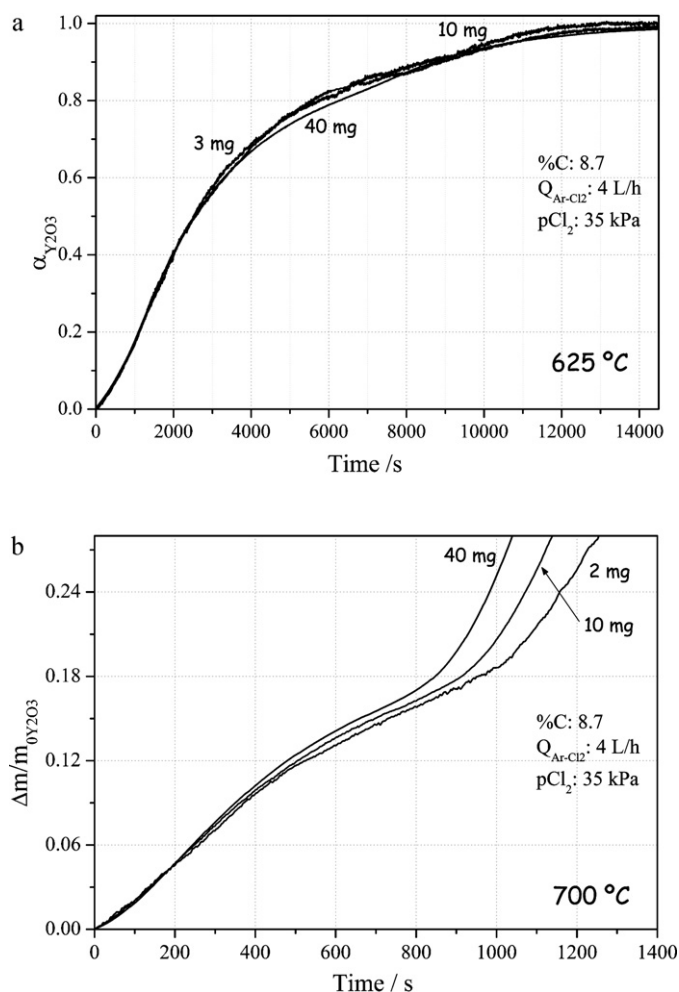
Fig. 4. Effect of the reaction bed thickness on reaction rate of chlorination of Y_2O_3–C (8.7%). (a) 625 °C and (b) 700 °C.

Fig. 5. Effect of chlorine partial pressure on the kinetics of chlorination of Y_2O_3–C (8.7%). (a) 625 °C and (b) 700 °C.

%C higher than stoichiometry of reaction (7) the system advances through *STAGE III* until the complete formation of the chloride. If the temperature is lower than Tf_{YCl_3} or %C lower than stoichiometry of reaction (7) a fraction of the YOCl produced through *STAGE I* is carbochlorated forming YCl_3 and the final product is composed by YOCl + YCl_3 (*STAGE III* does not occur).

Several kinetic studies of oxide–Cl_2–sucrose carbon systems have shown that the carbochlorination reaction has two stages: ZrO_2 [6,8], TiO_2 [9,10], Fe_2O_3 [11], $FeTiO_3$ [12]. The first stage is called fast and it is influenced by the gaseous intermediate species generated in the Cl_2–C interaction. The second one is denominated slow and the carbon acts thermodynamically, diminishing the oxygen potential. The stages fast and slow in these systems are equivalent to the *STAGES II* and *III* in the Y_2O_3–C–Cl_2 system.

3.2. STAGE I

3.2.1. Effect of the gas phase mass transfer

The overall rate in gas–solid reactions can be controlled by gas phase mass transfer by two processes: (1) reacting gas starvation and (2) convective mass transfer through the boundary layer [13,14]. The first process can be analyzed studying the effect of the total flow rate (Q_{Ar-Cl_2}) on the reaction rate. Fig. 3 shows the influence of Q_{Ar-Cl_2} at 625 and 700 °C, in a range of 2–8 L/h. The curves at 625 °C and 8.7%C show that the reaction rate at 2 L/h is a bit slower than the experiments at 4 and 8 L/h, and these two last curves have
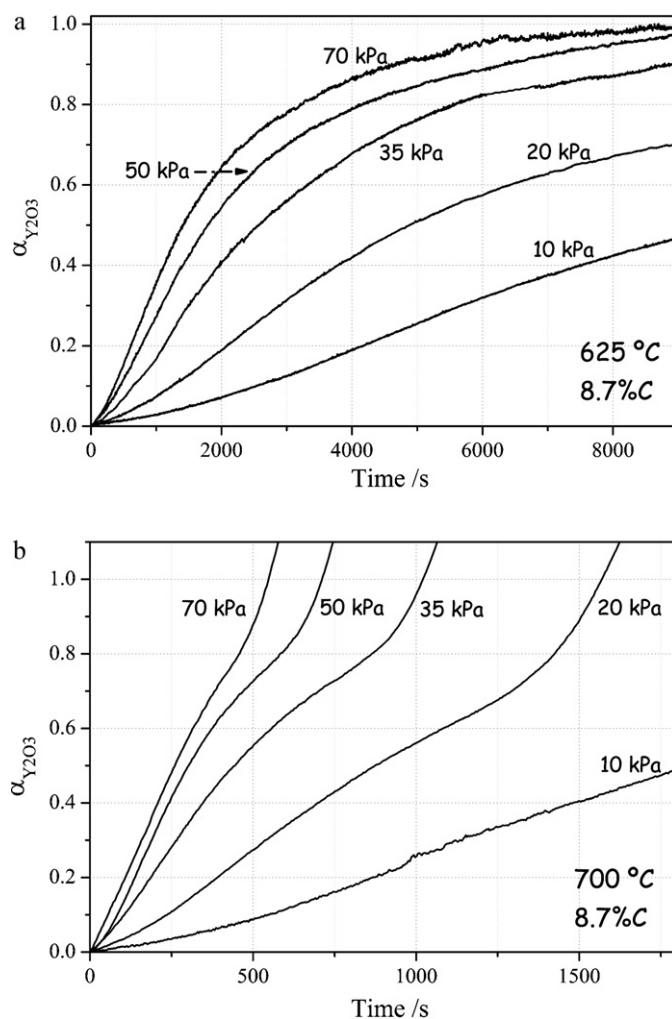
the same reaction rate. The conversion degree of *STAGE I* (α_{Y2O3}) is defined with respect to the consumption of Y_2O_3, according to the stoichiometry of reaction (1) ($w = 1.16$).

Fig. 3b shows thermogravimetries performed at 700 °C and 16.7%C at different Q_{Ar-Cl_2}. Curves at 675 and 725 °C are also shown to compare the effect of the temperature with respect to the influence of Q_{Ar-Cl_2}. It can be seen that the total flow rate has not an influence on the reaction rate of the *STAGE I* ($\Delta m/m_{0Y_2O_3} < 0.125$, which represents an $\alpha_{Y_2O_3} \approx 0.59$)

When the flow rate does not have an influence on the reaction rate it can be concluded that the system is not under conditions of reacting gas starvation. The experiments shown in Fig. 3 allow concluding that using $Q_{Ar-Cl_2} \geq 4$ L/h is high enough for avoiding starvation effects in the *STAGE I* of carbochlorination of Y_2O_3 at $T \leq 700$ °C, %C ≤ 16.7 and $pCl_2 \leq 35$ kPa.

The chlorine convective mass transfer through the boundary layer surrounding the sample is the other process in gas phase that can affect the reaction rate, even if the reacting gas starvation is absent. The molar flow of Cl_2 can be estimated by using the Ranz–Marshall correlation [15,16]:

$$h_D = \frac{D_{Ar-Cl_2} \cdot (2 + 0.6 \cdot N_{Re}^{1/2} \cdot N_{Sc}^{1/3})}{L} \tag{III}$$

where h_D is the mass transfer coefficient, D_{Ar-Cl_2} is the binary diffusion coefficient for Ar–Cl_2, $N_{Re} = U \cdot L/\nu$ represents the Reynolds number (U is the linear fluid velocity and ν is the kinematic vis-
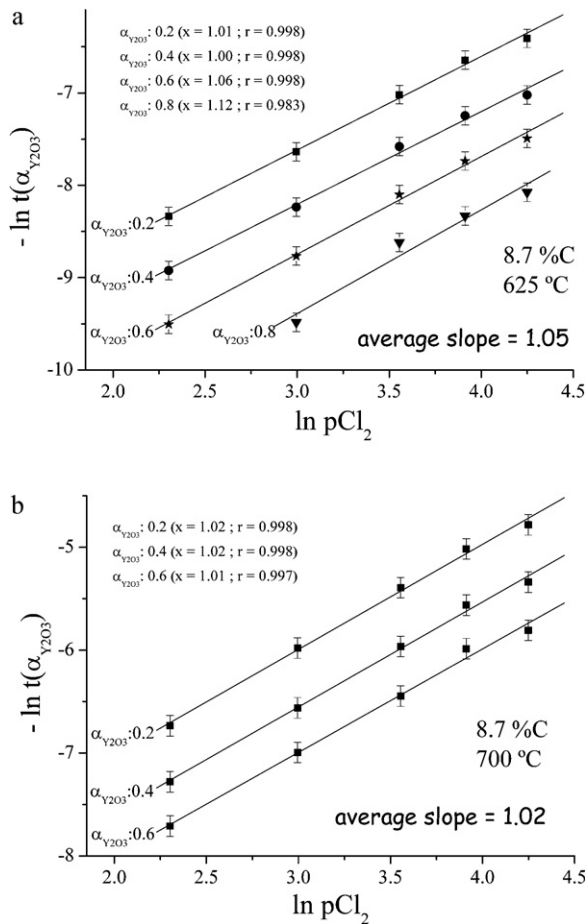
Fig. 6. Plot of Eq. (VIII) at various conversions in the *STAGE I*. (a) 625 °C and (b) 700 °C.

Fig. 7. Effect of temperature on chlorination of Y_2O_3–C (*STAGE I*). (a) 8.7%C and (b) 16.7%C.

cosity), $N_{sc} = \nu/D_{Ar-Cl_2}$ is the Schmidt number, and L is the sample characteristic dimension.

The rate at which mass is being transferred from the fluid to the solid per unit solid surface is given by:

$$N_{Cl_2} = \frac{1}{A} \cdot \frac{dn_{Cl_2}}{dt} = h_D \cdot (C_{Cl_2,0} - C_{Cl_2,S}) = \frac{h_D}{R_g \cdot T} \cdot (P_{Cl_2,0} - P_{Cl_2,S})$$
(IV)

where A is the sample external surface, dn_{Cl_2}/dt is the chlorine molar flow, C_{Cl_2} is the chlorine partial pressure, the subscripts 0 and S represent the bulk and sample surface, and R_g is the gas constant.

Combining Eqs. (III) and (IV):

$$\frac{dn_{Cl_2}}{dt} = \frac{D_{Ar-Cl_2} \cdot (2 + 0.6 \cdot N_{Re}^{1/2} \cdot N_{Sc}^{1/3})}{L} \cdot \frac{(P_{Cl_2,0} - P_{Cl_2,S})}{R_g \cdot T} \cdot A \quad (V)$$

The values of dn_{Cl_2}/dt calculated by Eq. (V) for temperatures between 600 and 800 °C and carbon contents of 8.7 and 16.7% are shown in Table 2. Reaction (1) can be assumed as irreversible since the values of the equilibrium constants are 2.54×10^{14} and 1.67×10^{11} at 600 and 800 °C, respectively ($w =$ 1.16, [7]). Therefore, the value of $P_{Cl_2,S}$ employed in the calculus is zero. The ν and D_{Ar-Cl_2} values were obtained from the Chapman–Enskog theory [13,17], and experimental conditions employed were $pCl_2 = P_{Cl_2,S}$: 35 kPa, Q_{Ar-Cl_2} : 4 L/h. The chlorine flows calculated by Eq. (V) are valid for a pellet in a freely flowing gas. Hills [14] and Hakvoort [18] proposed that the values obtained by the Ranz–Marshall correlation are more than one order of magnitude higher than the mass transfer rates into powders contained within crucibles. The criterion used in this work
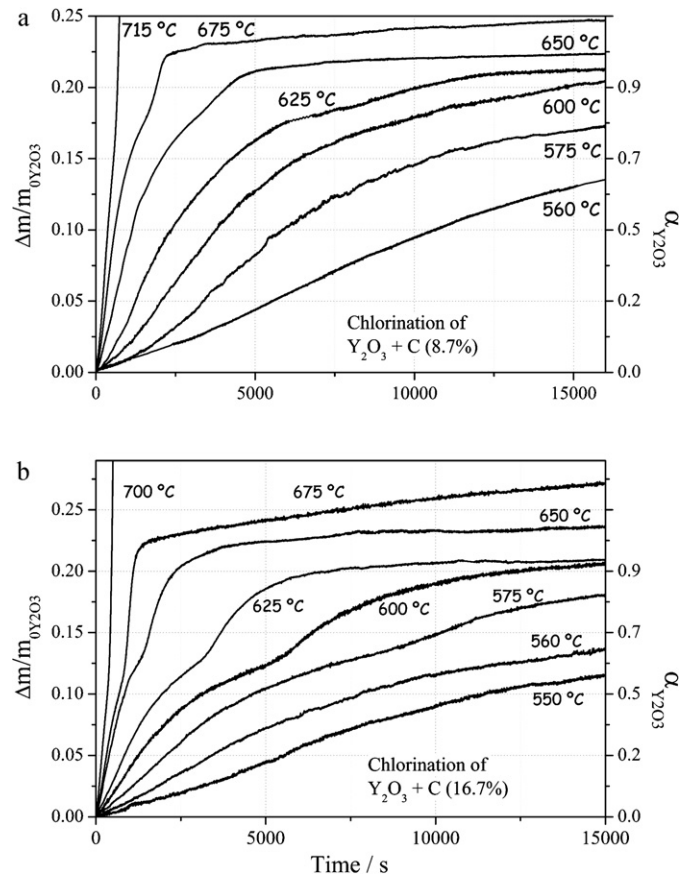
for conclude that the reaction rate is not influenced by the convective mass transfer is when the experimental rate is at least two orders of magnitude smaller than the rate calculated by Eq. (V).

The table also include the experimental chlorine molar flow calculated using the stoichiometry of reaction (1) with $w = 1.16$. The results show that for temperatures below 700 °C and carbon contents lower than 16.7%, the kinetics is not affected by the chlorine transfer through the boundary layer.

3.2.2. Analysis of mass transfer through the interparticle voids

The influence of the pore diffusion on the reaction rate was evaluated by varying the reaction bed thickness. For this, the sample mass was varied between 2 and 40 mg. Fig. 4a shows the effect of the sample mass in carbochlorinations performed at 625 °C and 8.7%C. The thermogravimetric curves show that the reaction kinetics does not depend on mass transfer through the sample pores. The effect of the sample mass at 700 °C and 8.7%C is shown in Fig. 4b. It can be seen that until the shoulder placed at $\Delta m/m_{0Y_2O_3} \approx 0.17$ (after which *STAGE II* begins) the curves are very similar, indicating that the sample mass has not influence on the kinetics of *STAGE I*. The effect of the reaction bed thickness was also analyzed at 700 °C and 16.7%C, obtaining the same result as 8.7%C.

3.2.3. Determination of the equation rate

The results discussed in the previous sections showed that gas phase and interparticle pore diffusion do not affect the kinetics of *STAGE I* at temperatures below 700 °C and carbon content of 8.7 and 16.7%. Therefore, the reaction is under chemical control and
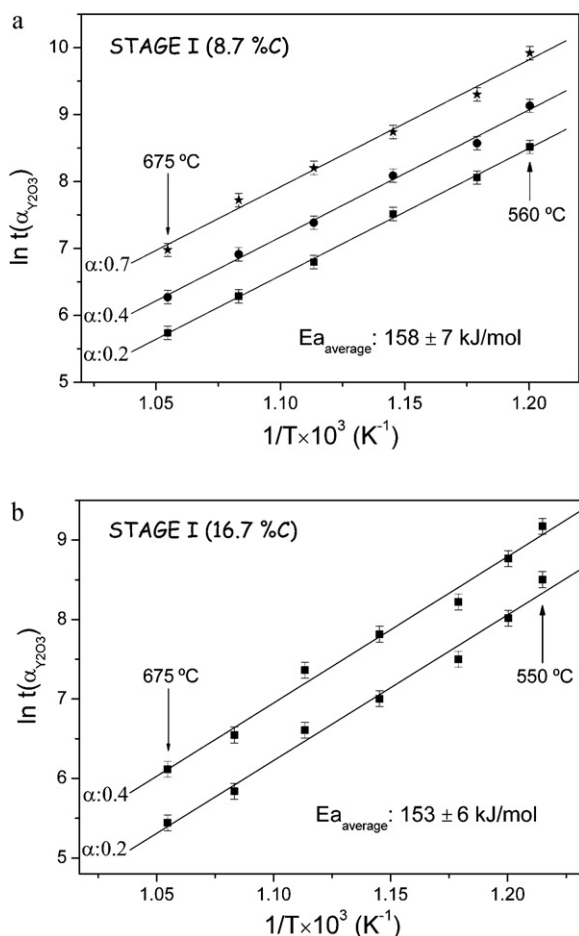
Fig. 8. Plot of $\ln t(\alpha)$ vs. $1/T$ (Eq. (IX)) at various conversions for *STAGE I* of Y_2O_3 carbochlorination. The stoichiometry considered corresponds to reaction (1) ($w = 1.16$). (a) 8.7%C and (b) 16.7%C.

the reaction rate can be expressed as follows

$$\frac{d\alpha}{dt} = k(T) \cdot F(pCl_2) \cdot G(\alpha) \qquad (VI)$$

where $k(T)$ refers to an Arrhenius equation, $F(pCl_2)$ expresses the dependence of reaction rate on pCl_2, and $G(\alpha)$ is a function that describes the geometric evolution of the solid reactant. The conversion degree is defined as

$$\alpha = \alpha_{Y_2O_3} = \frac{\Delta m}{m_0} \cdot \frac{1}{f} \qquad (VII)$$

where Δm is the mass change measured by the thermobalance at a given time, m_0 is the Y_2O_3 initial mass and f is the final relative mass change of reaction (1) ($f = 0.212$ for $w = 1.16$).

3.2.3.1. Reaction order with respect to the chlorine partial pressure. The effect of the chlorine partial pressure (pCl_2) on the reaction rate of carbochlorination of Y_2O_3 was studied at 625 and 700 °C, with 8.7%C, Q_{Ar-Cl_2}: 4 L/h, and m_0: 10 mg (Fig. 5). The range of pCl_2 analyzed was 10–70 kPa.

The procedure to obtain the reaction order with respect to the chlorine partial pressure is the following: Eq. (VI) is integrated, $F(pCl_2)$ is assumed as equal to $B \times pCl_2{}^x$ (where B is a constant and x is the reaction order with respect to pCl_2), temperature is maintained constant, and natural logarithms are applied. The expression obtained is

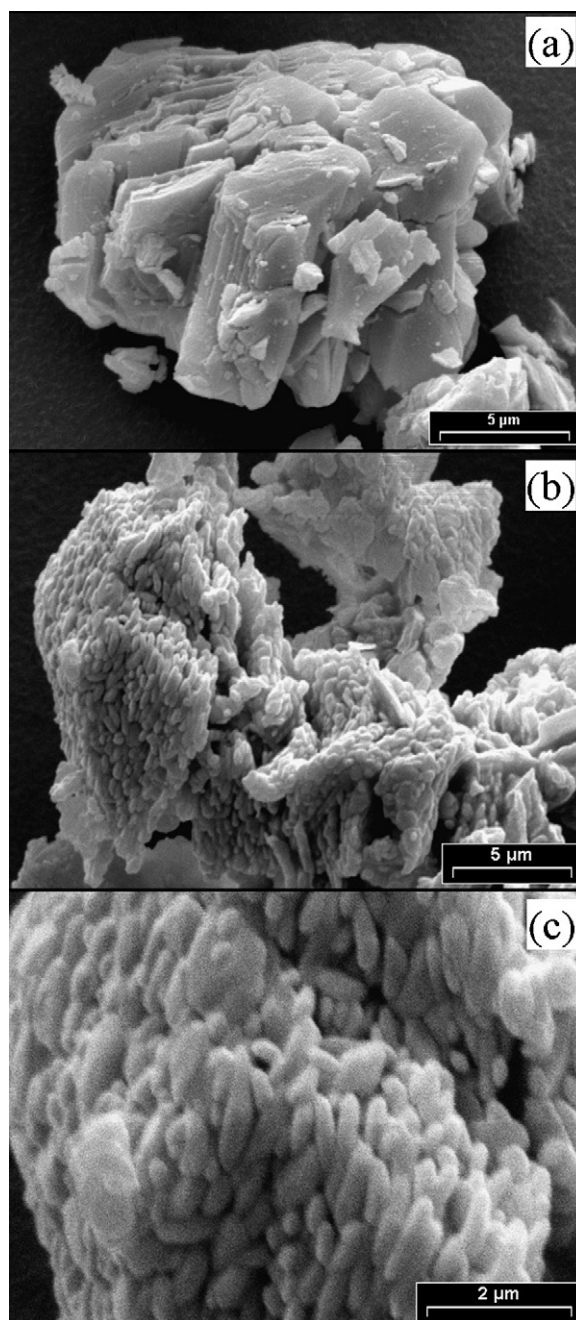$$-\ln t(\alpha) = H(\alpha) + x \ln pCl_2 \qquad (VIII)$$

Fig. 9. SEM images of: (a) unreacted Y_2O_3; (b) and (c) 675 °C, $\alpha_{Y_2O_3} = 1$.

where $t(\alpha)$ is the time at which the reaction reaches a conversion degree α at a given temperature and $H(\alpha)$ is a function that depends on α (since T is kept constant). The reaction order for a given α and T is obtained by plotting $-\ln t(\alpha)$ in function of $\ln pCl_2$ and calculating the slope of the curve. Fig. 6 shows the fits of Eq. (VIII) for the curves of Fig. 5, obtaining average reaction orders of 1.05 and 1.02 for 8.7 and 16.7%C. These values are very close to 1, which is the reaction order obtained for the direct chlorination of Y_2O_3 to produce YOCl [2]. It was considered an experimental scattering error of 10% in the time to reach a given conversion.

3.2.3.2. Effect of the temperature—activation energy. Fig. 7 shows the effect of the temperature on *STAGE I* of the chlorination of Y_2O_3–C in samples with 8.7 and 16.7%C at temperatures between 550 and 715 °C. The other experimental conditions were Q_{Ar-Cl_2}: 4 L/h, m_0: 10 mg and pCl_2: 35 kPa.

Table 2
Comparison between calculated and measured molar flow of chlorine for *STAGE I*.

T (°C)	D_{Ar-Cl_2} (cm²/s)	υ (cm²/s)	dn_{Cl_2}/dt [calculated] (mol Cl₂/s)[a]	dn_{Cl_2}/dt [experimental] (mol Cl₂/s)[b]		$(dn_{Cl_2}/dt)_{CALC}/(dn_{Cl_2}/dt)_{exp}$	
				8.7%C	16.7%C	8.7%C	16.7%C
600	0.76	0.64	5.46×10^{-6}	5.79×10^{-9}	6.27×10^{-9}	944	871
650	0.83	0.71	5.67×10^{-6}	1.77×10^{-8}	1.99×10^{-8}	320	285
700	0.92	0.77	5.88×10^{-6}	4.47×10^{-8}	5.50×10^{-8}	132	107
750	1	0.85	6.08×10^{-6}	1.20×10^{-7}	1.43×10^{-7}	51	42
800	1.09	0.92	6.27×10^{-6}	2.90×10^{-7}	4.01×10^{-7}	22	16

Data used for the calculus: $L = 0.74$ cm; $A = 0.43$ cm²; $pCl_2 = 35$ kPa; $Q_{Ar-Cl_2} = 4$ L/h.

[a] Calculated from Eq. (V).
[b] Obtained from the linear range of the thermogravimetric curves in *STAGE I* (stoichiometry of reaction (1) with $w = 1.16$).

The comparison of Fig. 7a and b evidence that *STAGE II* (carbochlorination of YOCl) starts at a lower value of $\Delta m/m_{0Y_2O_3}$ for the samples with higher carbon content. For instance, at 625 °C *STAGE II* begins at 0.14 and 0.19 for 16.7 and 8.7%C, respectively.

The activation energy (Ea) was calculated using the "model-free" method [19,20]: Eq. (VI) is integrated, $k(T)$ is assumed that follows an Arrhenius form, pCl_2 is a constant value, and natural logarithms are applied:

$$\ln t(\alpha) = C(\alpha) + \left(\frac{Ea}{R_g} \right) \frac{1}{T} \tag{IX}$$

where $C(\alpha)$ is a function that only depends on α (pCl_2 is constant). A plot of $\ln t(\alpha)$ vs. $1/T$ for a given α allow calculate Ea through the slope of the curve.

The curves of Fig. 7 were converted into conversion curves ($\alpha_{Y_2O_3}$ vs. t, right vertical axe) taking into account the stoichiometry of reaction (1) ($w = 1.16$). Fig. 8 shows the plots of Eq. (IX) for these conversion curves, being 675 °C the maximum temperature analyzed. This value was selected because at 700 °C the reaction of YOCl carbochlorination to form YCl₃ (*STAGE II*) is more feasible to occur since the chloride is in liquid state. The maximum values of α were 0.7 and 0.4 for 8.7 and 16.7%C, respectively. These maximum values were used to assure that the activation energy obtained belong to the *STAGE I*. The fit straight lines are practically parallels for every conversion value; this behaviour is indicating that the controlling mechanism is the same at all conversions analyzed. The values obtained for Ea were 158 ± 7 and 153 ± 6 kJ/mol for 8.7 and 16.7%C, respectively. The activation energies are practically the same and they are lower than the obtained by us using the

model-free method for the formation of YOCl by Y₂O₃ chlorination, which it was equal to 190 kJ/mol [2].

Data found in the literature for the formation of YOCl correspond to the reactive systems $YPO_4(s) + C(s) + Cl_2(g)$ [21] and $YPO_4(s) + CCl_4(g)$ [22]. The values for Ea reported by these authors are 75 and 47 kJ/mol, respectively. The reasons why these Ea are lower than those obtained by us can be related with the features of the reactive systems: Augusto and Oliveira [22] used $CCl_4(g)$ as chlorinating agent and Gimenes [21] used coal with a content of 56.5% (wt/wt, carbon mass/total mass). Besides, both authors used a rare-earth mineral (xenotime), particle size higher than 45 μm and sample mass higher than 100 mg.

3.2.3.3. Reaction model–determination of $G(\alpha)$. In the previous work we have determined that the reaction of formation of YOCl by Y₂O₃–C chlorination proceeds through a nucleation and growth mechanism [1]. Fig. 9 shows SEM images of (a) unreacted Y₂O₃ and (b and c) reacted sample at 675 °C until $\alpha_{Y_2O_3} = 1$.

The conversion curves were analyzed with Johnson–Mehl–Avrami model (JMA) [23–26], which describes this type of mechanism. The JMA description proposes that the expression of the conversion for isothermal transformations is the following

$$\alpha = 1 - \exp[-K(T)t]^n \tag{X}$$

$$K = K_0 \exp\left(\frac{-Ea}{R_g T} \right) \tag{XI}$$

where n is the JMA exponent, $K(T)$ is the rate constant, K_0 is the pre-exponential factor and Ea is the effective activation energy. The parameters n, K_0 and Ea depend on the nucleation and growth mechanisms.

The conversion curves of Fig. 7 were fitted with Eq. (X), and the values of n and K for each temperature and %C were obtained. The curves were carefully analyzed in order to fit only the *STAGE I* of the reaction. For this, the chlorination curves of mixtures with 8.7%C were fully fitted with the JMA model for $T \le 600$ °C, and until $\alpha_{Y_2O_3} = 0.75$ for $T \ge 625$ °C, whereas curves corresponding to 16.7%C were fully fitted for $T \le 575$ °C, and until $\alpha_{Y_2O_3} = 0.40$ for $T \ge 600$ °C ([1], Table 1).

The results for the mixture with 8.7%C are showed in Fig. 10. The experimental curves are showed as line graph and the calculated curves as scatter graph. The experimental curves were adequately fitted and the JMA parameters obtained were the following (Ea is calculated through the slope of the $\ln K$ vs. $1/T$ graph):

$8.7\%C \rightarrow n_{average}: 1.20 \pm 0.07; \quad Ea : 165 \pm 6$ kJ/mol

$16.7\%C \rightarrow n_{average}: 1.14 \pm 0.04; \quad Ea : 152 \pm 7$ kJ/mol

The values obtained for the effective Ea are in good agreement with those obtained by the model-free method (158 ± 7 and
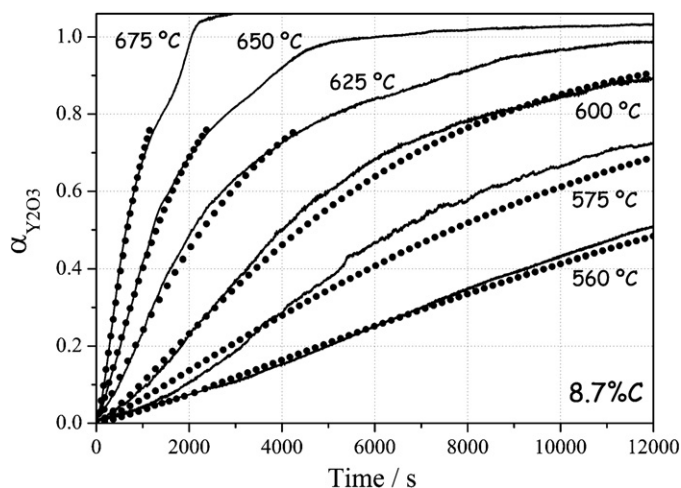

Fig. 10. Conversion curves of Fig. 7a (8.7%C) fitted with the JMA model. Line graphs: experimental curves; scatter graphs: calculated curves.

153 ± 6 kJ/mol, for 8.7 and 16.7%C, respectively). A discussion of the theoretical development of the JMA model is needed in order to understand the physical and kinetic significance of the JMA exponent (n) obtained. In principle, for isokinetic transformations n can only take specific values from the different nucleation and growth models [27]. However, Kempen et al. [28] demonstrated numerically that intermediate and temperature dependent values of JMA parameters are also possible for combination of the different nucleation models. The nucleation models considered are continuous nucleation and site saturation, whereas the growth models are volume diffusion and interface processes. Volume diffusion controlled growth can occur upon phase transformations where long range compositional changes take place. The case of interface controlled

Fig. 11. Effect of the reaction temperature on chlorination of Y_2O_3–C. (a) 8.7%C, (b) 16.7%C and (c) 30%C. Experimental conditions: pCl_2: 35 kPa, $Q_{Ar–Cl_2}$: 4 L/h, and m_0: 10 mg.

growth can occur in absence of compositional changes (allotropic phase transformations) [28]. Therefore, we can consider that the growth of YOCl nuclei is diffusion controlled. For this situation, n can take the following values: (1) between 1/2 (one-dimensional growth) and 3/2 (three-dimensional growth) for site saturation and (2) between 3/2 (one-dimensional growth) and 5/2 (three-dimensional growth) for continuous nucleation.

The n value in the reaction of YOCl formation by direct chlorination of Y_2O_3 calculate by us was equal to 1.51 ± 0.14 [2]. This value is compatible with an anisotropic growth of YOCl nuclei and continuous nucleation. In the Y_2O_3 carbochlorination the growth of YOCl nuclei are also anisotropic as can be observed in the SEM images of Fig. 9b and c. The JMA exponents obtained in the carbochlorinations are lower than those obtained by the direct chlorination and can be compatibles with a combination of nucleation models (site saturation and continuous nucleation) and anisotropic growth. In this case, n varies between 1/2 for site saturation and 3/2 for continuous nucleation. The addition of sucrose carbon in the Y_2O_3–Cl_2 system causes that a given number of YOCl nuclei are present at a time near to zero, and others nuclei are nucleated in a continuous form. The effective Ea value is affected by the activation energies associated to the nucleation and growth models. In the carbochlorination the nucleation is a combination of site saturation and continuous nucleation. The site saturation mechanism supposes that the number of supercritical nuclei does not change during the transformation; therefore all nuclei are present at zero time. Then, this mechanism is not an activated process and its Ea is zero. This behaviour explains the Ea decrease, from 187 kJ/mol for direct chlorination [2], to an average value of 158 kJ/mol for carbochlorination.

The expression for the function $G(\alpha)$ can be obtained by combining Eq. (VI) and (X):

$$G(\alpha) = n \cdot (1 - \alpha) \cdot [-\ln(1 - \alpha)]^{(n-1)/n} \qquad (XII)$$

with the following values of $n = 1.20$ (8.7%C) and 1.14 (16.7%C)

3.3. STAGES II–III

STAGES II and III of the overall reaction consist of the YOCl carbochlorination to produce YCl_3. The kinetic analysis of these stages is more complex than for STAGE I. STAGE II can begin at values of $\Delta m/m_{0Y_2O_3}$ lower than 0.19, which is the minimum for total conversion of Y_2O_3 into YOCl. Therefore, at a given conditions, there is an interval of reaction where STAGES I and II are simultaneous, complicating the kinetic study. STAGE III is observed for temperatures higher than melting point of yttrium trichloride. Then, the mass change in this stage is affected by two opposite effects: (1) mass gain due to the formation of liquid YCl_3 and (2) mass loss due to the YCl_3 evaporation.

In order to analyze the influence of gas mass transfer on reaction rate, the experimental mass gain rates were compared with chlorine molar flow rates calculated by Eq. (V) [13,15,16]. The results are showed in Tables 3 (STAGE II) and 4 (STAGE III). Data used for the calculus are the same than those used for STAGE I: $L = 0.74$ cm; $A = 0.43$ cm^2; $pCl_2 = 35$ kPa, $Q_{Ar–Cl_2} = 4$ L/h. The stoichiometry used was the same for both stages, and it was calculated from reactions (1) and (4) with $w = 1.16$ and $z = 4$ [1]. The results in Table 3 show that the calculated rates never were two orders of magnitude higher than the experimental rate (at 700 °C the ratio calculated/experimental rate is 53.9 and 15.2 for 8.7 and 16.7%C). Therefore, the reaction rate may be affected by the chlorine diffusion through the boundary layer surrounding the solid sample. The results for STAGE III (Table 4) indicate that for 16.7%C the convective chlorine transfer can be influencing the reaction kinetics in the whole temperature range of this stage. For 8.7%C, the reaction rate is not affected by the convective mass transfer for temperatures lower than 850 °C.
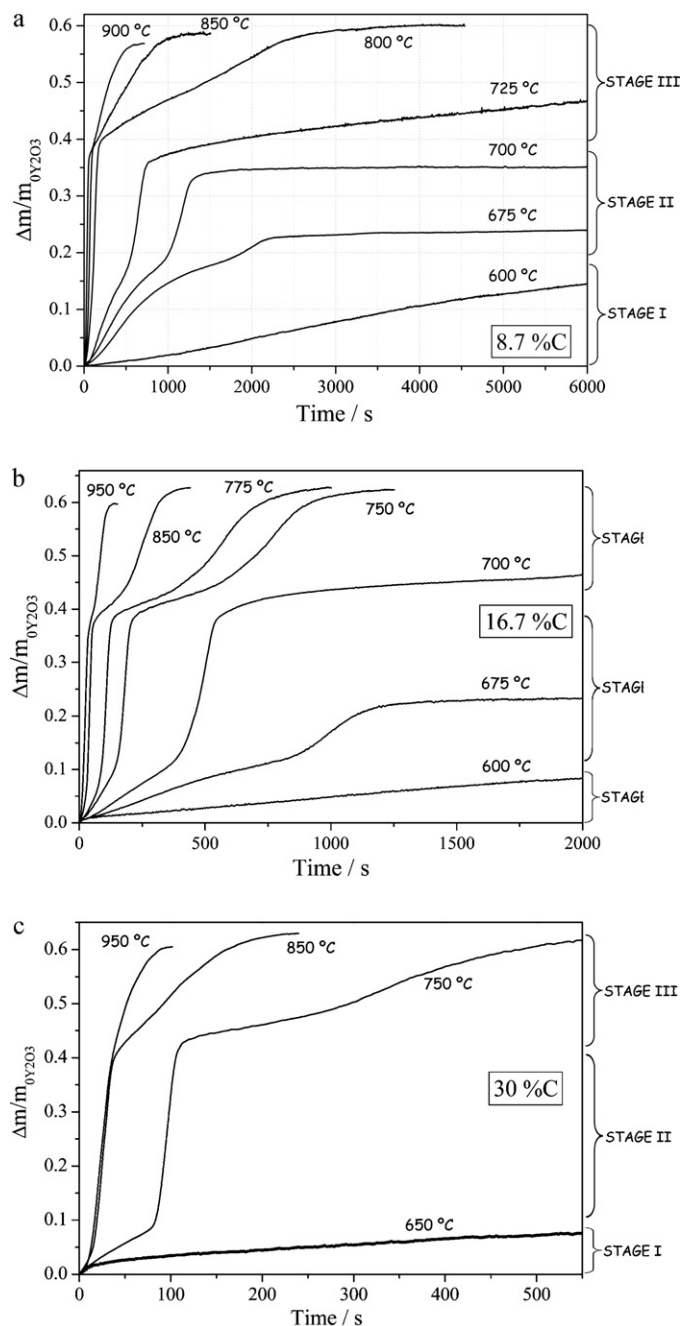
Table 3
Comparison between calculated and measured chlorine molar flow for *STAGE II*.

T (°C)	dn_{Cl_2}/dt [calculated] (mol Cl$_2$/s)[a]	dn_{Cl_2}/dt [experimental] (mol Cl$_2$/s)[b]		$(dn_{Cl_2}/dt)_{CALC}/(dn_{Cl_2}/dt)_{exp}$	
		8.7%C	16.7%C	8.7%C	16.7%C
700	5.88×10^{-6}	1.09×10^{-7}	3.87×10^{-7}	53.9	15.2
750	6.08×10^{-6}	0.375×10^{-6}	1.51×10^{-6}	16.2	4.0
800	6.27×10^{-6}	0.79×10^{-6}	2.24×10^{-6}	7.9	2.8
850	6.47×10^{-6}	1.38×10^{-6}	2.86×10^{-6}	4.7	2.3

[a] Calculated from Eq. (V).
[b] Obtained from the linear range of the thermogravimetric curves in *STAGE II* (stoichiometry of reaction (2) with $n = 1.42$).

Table 4
Comparison between calculated and measured chlorine molar flow for *STAGE III*.

T (°C)	dn_{Cl_2}/dt [calculated] (mol Cl$_2$/s)[a]	dn_{Cl_2}/dt [experimental] (mol Cl$_2$/s)[b]		$(dn_{Cl_2}/dt)_{CALC}/(dn_{Cl_2}/dt)_{exp}$	
		8.7%C	16.7%C	8.7%C	16.7%C
750	6.08×10^{-6}	4.9×10^{-9}	8.25×10^{-8}	1241	73.7
800	6.27×10^{-6}	1.37×10^{-8}	1.4×10^{-7}	457	44.8
850	6.47×10^{-6}	4.74×10^{-8}	2.4×10^{-7}	136	27
900	6.66×10^{-6}	1.06×10^{-7}	4.7×10^{-7}	62.8	14.2
950	6.84×10^{-6}	1.92×10^{-7}	7.3×10^{-7}	35.6	9.4

[a] Calculated from Eq. (V).
[b] Obtained from the linear range of the thermogravimetric curves in *STAGE III* in the zone of higher rate (stoichiometry of reaction (3) with $p = 1.42$).

The effect of the temperature on the Y$_2$O$_3$ carbochlorination kinetics is shown in Fig. 11 for the samples with carbon content of 8.7, 16.7 and 30%. The ranges of $\Delta m/m_{0Y_2O_3}$ corresponding at each stage are showed. The results analyzed above evidenced that the kinetics of *STAGE II* may be affected by the gas mass transfer. The kinetic behaviour of this stage in the curves of Fig. 11 agrees with this, because the slopes of *STAGE II* are almost independent of the temperature. In the carbochlorinations performed at 850 and 950 °C with 30%C the curves are practically the same for *STAGES I* and *II*, being different from the beginning of *STAGE III*.

4. Conclusions

The reaction kinetics of Y$_2$O$_3$-sucrose carbon chlorination was studied. The reaction proceeds through three successive stages until the formation of liquid YCl$_3$. The characterization and stoichiometry of the stages were determined by the authors in a previous paper. *STAGE I* corresponds to formation of solid YOCl and it was found that reaction is under chemical control for temperatures below 700 °C. The YOCl formation follows a nucleation and growth model and the conversion curves were analyzed with the Johnson–Mehl–Avrami description. The calculated curves fitted adequately the experimental data, obtaining values for n of 1.20 (8.7%C) and 1.14 (16.7%C). These JMA exponents are compatible with a combination of nucleation models (continuous nucleation and site saturation) and anisotropic growth controlled by diffusion. The effects of parameters evaluated can be expressed by global reaction rate equations for the two carbon contents analyzed:

$$\frac{d\alpha}{dt} = 1.9 \times 10^4 (\text{kPa seg})^{-1} \cdot \exp\left(-\frac{165\,\text{kJ mol}^{-1}}{R_g \cdot T}\right)$$
$$\cdot p\text{Cl}_2 \cdot \{1.20 \cdot (1-\alpha) \cdot [-\ln(1-\alpha)]\}^{1/6} \quad (8.7\%C)$$

$$\frac{d\alpha}{dt} = 8.4 \times 10^3 (\text{kPa seg})^{-1} \cdot \exp\left(-\frac{152\,\text{kJ mol}^{-1}}{R_g \cdot T}\right)$$
$$\cdot p\text{Cl}_2 \cdot \{1.14 \cdot (1-\alpha) \cdot [-\ln(1-\alpha)]\}^{0.123} \quad (16.7\%C)$$

The effective activation energy for *STAGE I* was also calculated by the model-free method, obtaining 158 and 153 kJ/mol for 8.7 and 16.7%C, respectively. These values are in good agreement with those obtained through an Arrhenius plot of the rate constants resulting of the JMA treatment.

It was not possible to obtain kinetic parameters of the *STAGES II* and *III*. *STAGE II* is the fastest of overall reaction and the kinetics is affected by gas mass transfer. The kinetic analysis showed that the rate of *STAGE III* is not affected by the gas phase diffusion for temperatures below to 850 °C (8.7%C). However, mass change in the *STAGE III* involves two opposite processes: mass gain produced by the formation of liquid YCl$_3$ and mass loss due to YCl$_3$ evaporation. Discrimination of these factors is required to obtain kinetic parameters.

References

[1] J.P. Gaviría, A.E. Bohé, Carbochlorination of yttrium oxide, Thermochim. Acta 509 (2010) 100–110.
[2] J.P. Gaviría, A.E. Bohé, The kinetics of the chlorination of yttrium oxide, Metall. Trans. B 40 (2009) 45–53.
[3] J. Gonzalez, M. del, C. Ruiz, A. Bohe, D.M. Pasquevich, Oxidation of carbons in the presence of chlorine, Carbon 37 (1999) 1979–1988.
[4] V.T. Amorebieta, A.J. Colussi, Direct study of the catalytic decomposition of chlorine and chloromethanes over carbon films, J. Phys. Chem. Kinet. 17 (1985) 849–858.
[5] D.M. Pasquevich, PhD Thesis, Facultad de Ciencias Exactas de la Universidad Nacional de La Plata, Argentina, 1990.
[6] D.M. Pasquevich, A.M. Caneiro, A thermogravimetric analyzer for corrosive atmospheres and its applications to the chlorination of ZrO$_2$–C mixture, Thermochim. Acta 156 (1989) 275–283.
[7] HSC 6.12, Chemistry for Windows, Outukumpu Research Oy, Pori, Finland, 2006.
[8] D.M. Pasquevich, J. Andrade Gamboa, A. Caneiro, On the role of carbon in the carbochlorination of refractory oxides, Thermochim. Acta 29 (1992) 209–222.
[9] J. Andrade Gamboa, A.E. Bohé, D.M. Pasquevich, Carbochlorination of TiO$_2$, Thermochim. Acta 334 (1–2) (1999) 131–139.

[10] J. Andrade Gamboa, D.M. Pasquevich, A model for the role of carbon on carbochlorination of TiO_2, Metall. Trans. B 31 (6) (2000) 1439–1446.
[11] F.C. Gennari, A.E. Bohé, D.M. Pasquevich, Effect of the reaction temperature on the chlorination of a Fe_2O_3–TiO_2–C mixture, Thermochim. Acta 302 (1–2) (1997) 53–61.
[12] G.G. Fouga, PhD Thesis, Instituto Balseiro – Universidad Nacional de Cuyo, Argentina, 2007.
[13] J. Szekely, J.W. Evans, H.Y. Sohn, Gas–Solid Reactions, Academic Press, USA, New York, 1976.
[14] A.W.D. Hills, The importance of convective mass transfer in the reduction of hematite, Metall. Trans. B 9 (1978) 121–128.
[15] W.E. Ranz, W.R. Marshall Jr., Evaporation from drops, Part I, Chem. Eng. Prog. 48 (3) (1952) 141–146.
[16] W.E. Ranz, W.R. Marshall Jr., Evaporation from drops, Part II, Chem. Eng. Prog. 48 (4) (1952) 173–180.
[17] G.H. Geiger, D.R. Poirier, Transport Phenomena in Metallurgy, Addison-Wesley, MA, USA, 1973.
[18] G. Hakvoort, TG measurement of gas–solid reactions, the effect of the shape of the crucible on the measured rate, Thermochim. Acta 233 (1994) 63–73.
[19] J.H. Flynn, Thermal analysis kinetics-problems, pitfalls and how to deal with them, J. Therm. Anal. 34 (1988) 367–381.
[20] S. Vyazovkin, Computational aspects of kinetic analysis. Part C. The ICTAC Kinetics Project – the light at the end of the tunnel? Thermochim. Acta 355 (2000) 155–163.
[21] M. Gimenes, H. Oliveira, Microstructural studies and carbochlorination kinetics of xenotime ore, Metall. Trans. B 32 (2001) 1007–1013.
[22] E.B. Augusto, H.P. Oliveira, Kinetics of chlorination and microstructural changes of xenotime by carbon tetrachloride, Metall. Trans. B 32 (2001) 783–791.
[23] M. Avrami, Kinetics of phase change. I. General theory, J. Chem. Phys. 7 (12) (1939) 1103–1113.
[24] M. Avrami, Kinetics of phase change. II. Transformation-time relations for random distribution of nuclei, J. Chem. Phys. 8 (2) (1940) 212–224.
[25] M. Avrami, Kinetics of phase change. III. Granulation, phase change, and microstructure, J Chem. Phys. 9 (2) (1941) 177–184.
[26] W.A. Johnson, R.F. Mehl, Reaction kinetics in process of nucleation and growth, Trans. Am. Inst. Min. Metall. Engs. 135 (1939) 416–427.
[27] J.W. Christian, The Theory of Transformations in Metals and Alloys, Pergamon Press, United Kingdom, Oxford, 1965.
[28] A.T.W. Kempen, F. Sommer, E.J. Mittemeijer, Determination and interpretation of isothermal and non-isothermal transformation kinetics; the effective activation energies in terms of nucleation and growth, J. Mater. Sci. 37 (2) (2002) 1321–1332.